

## RESEARCH ARTICLE

# Modelling and multiobjective optimization analysis of a permanent magnet synchronous motor design

Y. L. Karnavas  | I. D. Chasiotis | C. D. Korkas | S. K. Amoutzidis

Laboratory of Electrical Machines, Department of Electrical and Computer Engineering, Democritus University of Thrace, Xanthi, 671 00, Greece

**Correspondence**

Yannis L. Karnavas, Lab. of Electrical Machines, Department of Electrical and Computer Engineering, Room 0.21, Build. B, Democritus University of Thrace, Kimmeria, Xanthi, 671 00, Greece.

Email: karnavas@ee.duth.gr

**Abstract**

An alternative to traditional low-speed/high-torque drive systems, which are currently used in industry, could be the use of a permanent magnet synchronous motor directly coupled to the load and running at low speed, instead of the induction motor along with its mechanical transmission parts. The paper—in this context—deals with the analytical design procedure, optimization, and evaluation of such a motor (5 kW/50 rpm) and focuses on 2 topologies, ie, with inner and outer rotor. Finite element method designs of the permanent magnet machines are implemented as solutions of a complex optimization problem and several goals (multiobjectives) are considered (ie, machine weight minimization or efficiency maximization) with respect to relevant constraints. Three optimization methods are adopted and applied and a weighted cost function is proposed. The effectiveness of our problem design formulation approach and the use of these methods, in finding alternative and competitive permanent magnet synchronous motor designs, are also evaluated. The results reveal satisfactory design solutions and present acceptable performance. Moreover, by means of simulations, the application of several commercially available ferromagnetic materials for the motors' stator and rotor cores is performed. Last but not least, the effect of pole-arc per pole-pitch ratio along with the magnets length variation is also investigated.

**KEYWORDS**

computer aided design, finite element method, modelling and optimization, permanent magnet synchronous motors

## 1 | INTRODUCTION

Approximately 65% of the energy consumption in industrial sector worldwide is currently covered by a large number of induction motors used. The traditional mechanical transmission systems of low-speed/high-torque drive systems used (between the induction motor and the load), consist of camshafts or pulleys/belts, gear heads, and gears. It is evident, however, that the maintenance needs, the relative high cost and the possible deficiency of these drive systems are the main drawbacks of these setups. Low-cost and high-efficiency electrical drives are desirable since the economy plays an important role, on the one hand, and the environmental concern increases, on the other.<sup>1,2</sup> Thus, an attractive alternative of the induction motor-gearbox systems can be

their replacement with permanent magnet synchronous motor (PMSM). This can be justified by several reasons: (1) low speeds, ie, under 500 rpm allow the elimination of gearboxes, (2) since PMSM have no rotor winding they present higher efficiencies, (3) PMSM present lower noise levels and lower power consumption, (4) the PMSM line current is related to torque in a proportional way so it is possible to set the desired torque directly from current measurements (this cannot be done with induction motors), (5) the starting torque produced by PMSM is very high, (6) the magnetic materials used in PMSM are of relative low price.<sup>3</sup> There are many applications areas, which reveal the importance of research efforts for effective Computer Aided Design/Finite Element Analysis (CAD/FEA) optimization for PMSMs. Typical direct driven low-speed applications, which permanent

magnet (PM) machines already, include waste-water treatment plants, boat propulsion, wind turbines, and elevators. A PMSM for a mixer in direct-drive mode for waste-water plant has been studied.<sup>3,4</sup> Elevator application PM machine has also been presented.<sup>5</sup> Wind turbines also in direct-drive mode incorporating PMSM have been previously studied.<sup>6–9</sup> The design of a 100 kW PMSM for boat propulsion system has also been proposed.<sup>10</sup> A spoke magnet direct-drive PMSM with outer rotor has been also proposed recently.<sup>11</sup>

The paper aims to provide a rigorous insight in the PMSM design modelling and optimization problem through finite element method (FEM) as well as to investigate the effectiveness of specific optimization algorithms regarding their ability to find solutions of PMSM designs (as competitive alternatives) to replace conventional industrial gearbox-low speed drive systems equipped with induction motors. The work performs also a systematic parametric investigation aiming to determine (1) the effects of certain variables variation and (2) the influence of the core material used, to the reached optimized PMSMs. The organization of the work is as follows: The relative geometrical topologies and the necessary mathematical background of the overall motor design procedure are presented at Section 2, while the adopted

and applied optimization methods as well as the problem formulation are presented in Section 3. In the same section, the relevant constraints, the constant quantities, the categorization of the design variables, the proposed multiobjective cost functions are described. The corresponding analytical optimization results are shown in Section 4. Moreover, the work examines the application of 22 commercially available ferromagnetic materials for PMSM's stator/rotor cores and their influence on its efficiency as well as its weight. Finally, through a large number of simulations, the variation of (1) the pole arc to pole pitch ratio and (2) the PM length is investigated as per their effect on several quantities of major concern. All the above relevant design results are discussed and commented at the same section, while Section 5 concludes the work.

## 2 | RADIAL FLUX PMSM UNDER EXAMINATION

In radial flux PMSM, the current flows axially, while the magnetic flux flows radially inside them. Figure 1 depicts a generic cross section as well as detailed geometrical representations of the configurations under study.<sup>4</sup>

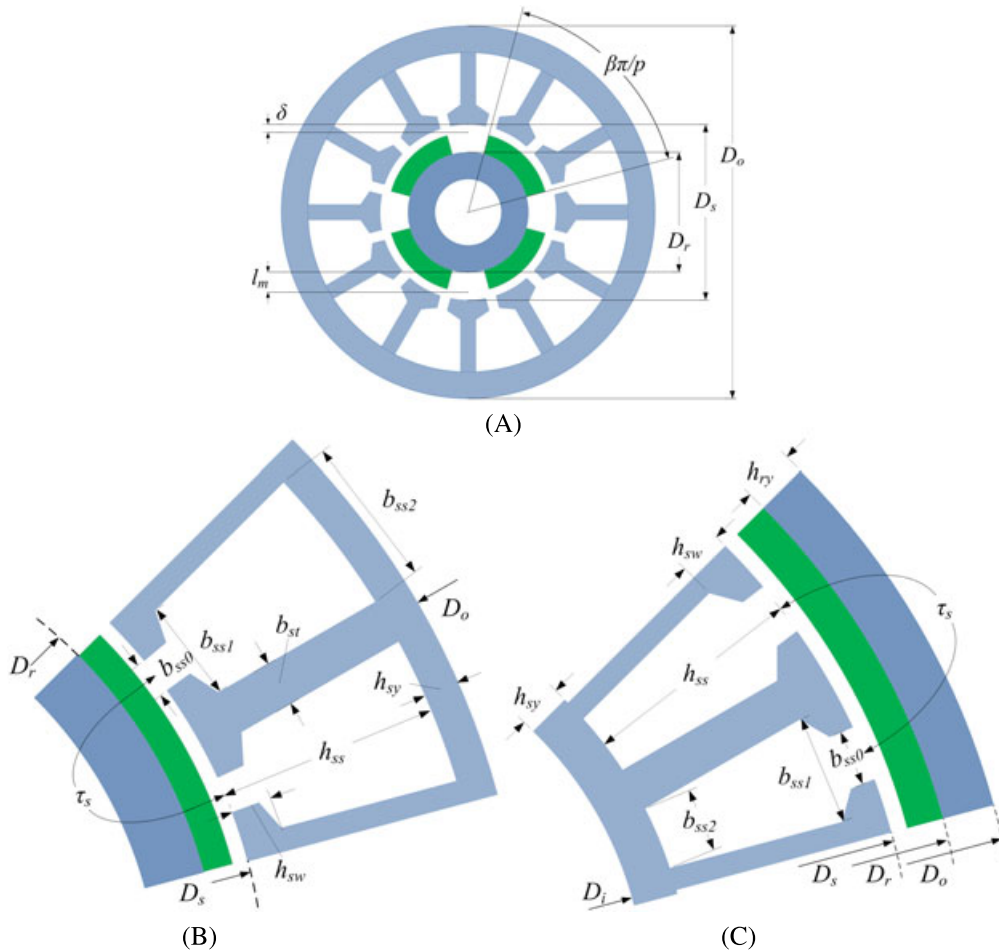


**FIGURE 1** Geometrical representations for the permanent magnet synchronous motor designs under study. A, General cross section (inner rotor). B, Detailed slot geometry (1 pole pair) with inner rotor configuration. C, Detailed slot geometry (1 pole pair) outer rotor configuration

In particular, Figure 1A depicts a geometrical overview of a PMSM with inner rotor configuration. Dimensions shown are the magnet length ( $l_m$ ), the pole arc to pole pitch ratio ( $\beta$ ) (also called *embrace*), the length of the airgap ( $\delta$ ), the inner diameter of the stator diameter ( $D_s$ ), the diameter of the rotor ( $D_r$ ), and the outer machine diameter ( $D_o$ ). Inner rotor means that the PMs are placed on the rotor surface (on the outer diameter of the rotor  $D_r$ ). By examining this topology closer, with respect to 1 pole pair, we consider a detailed slot representation for the motor, which is seen in Figure 1B. The figure reveals more geometrical parameters, which are needed for our analysis. In this figure, the quantities  $b_{ss0}$ ,  $b_{ss1}$ ,  $b_{ss2}$ , and  $b_{st}$  refer widths (bores) of the stator slot, while the quantities  $h_{sw}$ ,  $h_{ss}$  and  $h_{sy}$ , refer to the heights of the stator slot. The PMSM configuration with outer rotor turns out if the PMs are placed in the inner rotor circumference. In this case, the stator exists in the machine's centre, while the rotor covers the outer part of it. The latter detailed slot representation is given in Figure 1C. Although, both configurations have “pros” and “cons,” the first one seems to be the most preferable up to now from an industrial perspective. Nevertheless, this study is challenged to deal with the optimization of both configurations.

## 2.1 | Inner and outer rotor PMSM topology

In the first place, the ratio of the opening of the stator slot to its width is defined,

$$k_{\text{open}} = b_{ss0}/b_{ss1}. \quad (1)$$

Then, the slot pitch  $\tau_s$  is calculated (denoting the stator slots number as  $Q_s$ ),

$$\tau_s = \pi D_s / Q_s. \quad (2)$$

Considering the configuration of inner rotor (Figure 1B) the following relationships are obtained

$$D_s = 2(\delta + l_m) + D_r, \quad (3)$$

$$b_{ss1} = \pi \frac{D_s + 2h_{sw}}{Q_s} - b_{st}, \quad (4)$$

$$b_{ss2} = \pi \frac{D_s + 2h_{ss}}{Q_s} - b_{st}, \quad (5)$$

$$h_{sy} = \frac{1}{2} (D_o - (D_s + 2h_{ss})). \quad (6)$$

The area of the slot  $A_s$  can be computed as

$$A_s = \frac{1}{2} (b_{ss2} + b_{ss1}) (h_{ss} - h_{sw}). \quad (7)$$

In the same way, for the configuration of the outer rotor (Figure 1C) the subsequent equations can be obtained

$$D_s = D_r - 2(l_m + \delta), \quad (8)$$

$$b_{ss1} = \pi \frac{D_s - 2h_{sw}}{Q_s} - b_{st}, \quad (9)$$

$$b_{ss2} = \pi \frac{D_s - 2h_{ss}}{Q_s} - b_{st}, \quad (10)$$

$$h_{sy} = \frac{1}{2} (D_s - (D_i + 2h_{ss})), \quad (11)$$

$$h_{ry} = \frac{1}{2} (D_o - D_r). \quad (12)$$

It should be stated here that, for both configurations, the widths of the slots shown in Equations 4 to 5 and Equations 9 to 10, are considered as straight lines (and not arcs as they actually are), because the inner diameter of the stator  $D_s$  compared to the pitch of the slot  $\tau_s$  is large enough.

## 2.2 | Magnetic properties considerations of PMSM

The calculation of the maximum value  $B_m$  (amplitude) of the fundamental component of air-gap flux density shall be conducted next. Given the Carter factor by Equation 13, this can be calculated by Equation 14 since in PMSM designs the shape of flux density waveform is assumed to be rectangular, with width as wide as this of the magnets<sup>3</sup>:

$$k_C = \tau_s \left( \tau_s - \frac{(k_{\text{open}} b_{ss1})^2}{k_{\text{open}} b_{ss1} + 5\delta} \right)^{-1}, \quad (13)$$

$$B_m = B_r k_{\text{leak}} \left( 1 + \frac{\mu_r \delta k_C}{l_m} \right)^{-1}, \quad (14)$$

where  $\mu_r$  the relative permeability of the magnets,  $k_{\text{leak}}$  express the flux lines flowing through the air-gap (in percent)—called leakage factor—and  $B_r$  is the magnet's remanence flux density. By performing magnetostatic FEM simulations, it is easy to obtain the leakage factor. In this way, a simple although accurate linear relationship of  $k_{\text{leak}}$  regarding the PMSM poles  $p$  can be used<sup>12</sup>

$$k_{\text{leak}} = (100 - (7p/60 - c)) / 100. \quad (15)$$

Constant  $c$  has been found to be 3.0 and 0.5 for PMSM with outer and inner rotor configuration, respectively. Lastly, the iron losses of the ferromagnetic material should be considered. It is known that these losses can be split into eddy current losses and hysteresis losses,

$$P_{\text{fe}} = k_h f B_{sy}^\alpha + k_e f^2 B_{sy}^2, \quad (16)$$

where  $B_{sy}$  is the peak flux density of the stator,  $P_{\text{fe}}$  are the losses corresponding to iron,  $f$  is the frequency of the supply voltage,  $\alpha$ ,  $k_h$ , and  $k_e$  are the ferromagnetic material's coefficients, which can be obtained from its loss data. The importance of the stator core loss minimization in PMSM

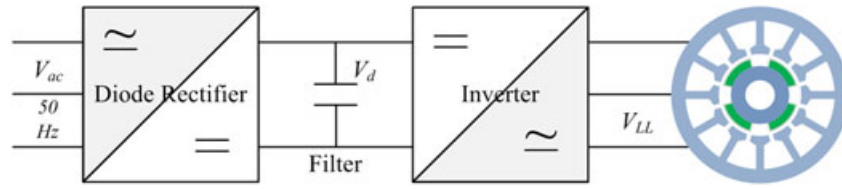


FIGURE 2 Typical permanent magnet motors drive setup

(through the optimization of the rotor geometry) can be justified, by observing Equation 16. Because of the frequency square proportionality of the eddy current losses, the latter dominate in high speeds only. However, the hysteresis losses are prevail here, because the frequency used in our cases is higher than its fundamental component.

### 2.3 | Electrical properties considerations of PMSM

Continuing, specific electrical parameters of the PMSM should be calculated. These include the supply and induced voltages, the resistance (per phase) of the stator windings, the current density, the ampere-turns, and the relevant inductances. It should be noted that PMSM machines are nonsalient ones, so  $q = 1$  and  $L_d = L_q$ .<sup>13</sup> Using the d-q axes analysis vector diagram (where  $I_q = I$ ), the phase supply voltage is

$$V = \sqrt{(|E| + R|I_q|)^2 + (L_d \omega |I_q|)^2}. \quad (17)$$

In hardware terms, this voltage corresponds to the output voltage of the inverter used (Figure 2). Considering a scenario with modulation ratio ( $m_a$ ) of 80% and a given capacitor DC voltage ( $V_d$ ), then  $V_{LL} = 0.612 m_a V_d$ . Thus,  $V_{LL}$  is approximately taken here as 195.8 V. The inverter's output frequency should be altered appropriately also for each geometry.<sup>14</sup>

Based on the PMSM geometry, the *rms* value of the induced voltage is now given by

$$E = \omega k_{w1} q n_s B_m L (D_s - \delta) / \sqrt{2}, \quad (18)$$

and the corresponding ampere-turns due to current peak loading are

$$n_s I = \frac{4T}{\pi (D_s - \delta)^2 L B_\delta k_{w1} k_{sl}} \tau_s, \quad (19)$$

where  $k_{sl}$  takes the values 0.95 and 0.94, respectively, for configurations of inner and outer rotor and is actually a compensating factor for the slot leakage losses. Now, the current density can be obtained as

$$J = n_s I / A_s f_s. \quad (20)$$

Additionally, the phase resistance of the stator's winding can be derived by

$$R = \frac{\rho_{Cu} n_s^2 q \{pL + k_{ew} \pi (D_s + h_{ss})\}}{f_s A_s}, \quad (21)$$

where for distributed windings the slot fill factor  $f_s$  is 0.45 and  $k_{ew}$  is a factor, which takes into account the end-windings influence.<sup>15</sup> The remaining variables in the Equations 18 to 21 are the active length of the machine ( $L$ ), the fundamental winding-factor ( $k_{w1}$ ), the coefficient of the permeance of the slot opening ( $\lambda_1$ ), the number of the conductors-per-slot ( $n_s$ ), and the number of slots/pole/phase ( $q$ ). Finally, the following equations can produce the values of the d-q magnetizing inductances ( $L_{md}$ ,  $L_{mq}$ ), the d-q inductances ( $(L_d, L_q)$ ), and the leakage inductance ( $L_l$ ).

$$L_d = L_q = L_l + L_{md} = L_l + L_{mq}, \quad (22)$$

$$L_l = p q n_s^2 L \mu_0 \lambda_1, \quad (23)$$

$$L_{md} = L_{mq} = \frac{3}{\pi} (q n_s k_{w1})^2 \frac{\mu_0}{\delta k_C + l_m / \mu_r} (D_s - \delta) L. \quad (24)$$

### 2.4 | Thermal considerations of PMSM

Generally, iron losses along with copper losses as heat sources and the geometry of the motor, are affecting its thermal behavior. Computational fluid dynamics and finite element analysis comprise the most used techniques for PMSM thermal studies. Lumped parameters circuit is another method and it is often preferred for its speed advantage. Other, more recent, thermal analysis techniques have been proposed also.<sup>16</sup> An in-depth thermal analysis study is beyond this work's scope. Instead, results of the relative slot current density calculation (Equation 20) will be derived, from which qualitative but safe conclusions can be extracted. Each (maximum) value of the slot current density ( $J_{\max}$ ), for every geometry, has to be up to a maximum allowable value. This value has been set as 800 A/cm<sup>2</sup> if the motor operates as an air-cooled one. For force-cooled PMSMs, this value<sup>17</sup> may exceed 1 kA/cm<sup>2</sup>.

## 3 | PROBLEM FORMULATION AND OPTIMIZATION METHODS USED

### 3.1 | Problem formulation

Many optimization problems (including electrical machines design) that need to be solved nowadays are in essence tasks that involve more than one objective. When the system engineer wants to optimize more than 1 objective at the same time, it is not always clear from the problem description (if any)

how to achieve this and how the objectives influence each other. Also, it is often not sufficient to try to optimize just 1 objective without considering the effect that this maximization has on the other objectives in the system. In such cases, we are dealing with a genuine multiobjective optimization problem. Formally, multiobjective optimization is the process of simultaneously optimizing multiple objectives which can be complementary, conflicting as well as independent. Thus, the goal of multiobjective optimization in electrical machines design is to search the variables space and eventually find variables values that provide different trade-offs between objectives. Usually, a (weighted) linear scalarization function is used to translate the original multiobjective problem into a single-objective problem that can be solved by single-objective techniques. The weight parameters  $\gamma_i \in [0, 1]$  are preference factors that identify the relative importance of objectives  $m$ , with  $\sum_{m=0}^{m-1} \gamma_i = 1$  for  $m$  objectives. This transforms the original problem into a single-objective optimization problem, which is a weighted convex sum of the original objectives:  $f(x) = \sum_{m=0}^{m-1} \gamma_i f_m(x)$ . This kind of scalarization imposes the problem where an even distribution of weights does not ensure an even distribution of solutions in the Pareto front. These limitations might not be crucial in practice for electrical machine design; since the Pareto front is often convex, the obtained solutions are just approximations to the optimal, and designers do not seek an even spread of solutions in the Pareto front. Nonetheless, it has been shown in the recent literature that such a simple multiobjective approach based on single-objective optimization algorithms is still inferior in practice to an multiobjective optimization approaches not relying on scalarizations.<sup>18</sup> It is evident from the above considerations as well as from Section 2 that the modelling procedure should take into account: (1) the available data of the PMSM design problem, (2) its constraints, (3) the objective function(s), and (4) the particularities of the solution method(s), by making choices in a careful manner. Here, a 5-kW/50-rpm waste-water treatment plant mixer motor is chosen,<sup>19</sup> since the goal of this work is to determine suitable PMSMs as replacements of a real worlds “induction motor-gearbox” system. The operating characteristics of the latter, and the corresponding desired ones of the PMSM under investigation, are shown in the Appendix (Table A1). Moreover, all the relevant information as well as the results obtained here will be presented in a tabular form due to the large number of variable names, symbols, etc.

### 3.1.1 | Design variables, constants and problem constraints

Continuing, the design variables selection follows. From Equations 1 to 24 and Figure 1, twelve design variables are chosen for optimization by the applied algorithms and are shown in Table A2. It should be noted that all of them refer to the motor geometry. Also, the use of the above equations have to be implemented into the algorithms for the implicit

calculation of all the other variables. The lower/upper bounds of these variables are shown in the same table. Moreover, the constant values used in the calculations are summarized in Table A3, while the relative problem constraints are presented in Table A4.

### 3.1.2 | Proposed objective function

Potential objectives in any machine design problem, and consequently in the PMSM one, may be quite a lot (ie, weight, and cost). To keep the complexity low, we proposed, here, a simple multiobjective formulation of the cost function to be minimized (Equations 25-26):

$$CF_j = \gamma_i \cdot Q_i, \quad (25)$$

where  $\gamma_i$  is a  $1 \times i$  row matrix, which contains the weight coefficients of the cost function and  $Q_i$  is a  $i \times 1$  column matrix, which contains the values of any PMSM quantities under optimization. Although this proposed formulation can be expanded to many variables, the quantities chosen here are 3 ( $i = 3$ ), namely, (1) the total machine weight ( $M_w^{tot}$ ), (2) the total magnets weight ( $M_m^{tot}$ ), and (3) the total copper losses ( $P_L^{tot}$ ). The weighting variations examined are also 3 ( $j = 3$ ) as shown in Equation 26.

$$\begin{aligned} CF_1 &= [0.70 \ 0.15 \ 0.15] \cdot [M_w^{tot} \ P_L^{tot} \ M_m^{tot}]^T \\ CF_2 &= [0.15 \ 0.70 \ 0.15] \cdot [M_w^{tot} \ P_L^{tot} \ M_m^{tot}]^T \\ CF_3 &= [0.15 \ 0.15 \ 0.70] \cdot [M_w^{tot} \ P_L^{tot} \ M_m^{tot}]^T. \end{aligned} \quad (26)$$

Regarding the selection of weights, a semiexhaustive search was implemented primarily in this work to explore the weight search space for linear scalarization and consequently to identify efficient weight combinations located on convex regions of the Pareto optimal set. This choice is justified because the current techniques that aim to identify or approximate convex regions in the Pareto optimal set are mainly limited to model-based or batch-learning approaches (which are, furthermore, not easily extendible to higher dimensional spaces, ie, problems with 3 or more objectives).

### 3.2 | Optimization methods applied

It can be easily seen that the considered PMSM designs are actually refer to a non-linear-constrained optimization problem, which in its general form can be expressed as

$$\min_{\mathbf{x}} F(\mathbf{x}) \quad \text{subject to} \quad H(\mathbf{x}) = 0, G(\mathbf{x}) \leq 0, \quad (27)$$

where  $H(\mathbf{x})$  and  $G(\mathbf{x})$  are the equalities and inequalities constraint sets, respectively. In algorithmic modelling terms, the problem can be implemented as finding the minimum of a function,

$$\min F(\mathbf{x})$$

$$\text{such that } C(\mathbf{x}) \leq 0, \quad C^{eq}(\mathbf{x}) = 0, \quad \mathbf{Ax} \leq \mathbf{b}, \quad \mathbf{A}^{eq}\mathbf{x} = \mathbf{b}^{eq},$$

$$\mathbf{l}^b \leq \mathbf{x} \leq \mathbf{u}^b$$

$$(28)$$

where



$\mathbf{A}$  and  $\mathbf{A}^{eq}$  are matrices,  $\mathbf{x}$ ,  $\mathbf{b}$ ,  $\mathbf{b}^{eq}$ ,  $\mathbf{l}^b$ , and  $\mathbf{u}^b$  are vectors;  $C(\mathbf{x})$  and  $C^{eq}(\mathbf{x})$  are functions, which return vectors; and  $F(\mathbf{x})$  is a function that returns a scalar. Finally,  $F(\mathbf{x})$ ,  $C(\mathbf{x})$ , and  $C^{eq}(\mathbf{x})$  can be nonlinear functions. Three optimization methods were chosen and applied here for solving our problem expressed in the form of Equation 28. These are (1) Fmincon (FMC), (2) genetic algorithm (GA), and (3) pattern search (PS). These techniques have been proved robust and efficient enough to most engineering problems in the past. Moreover, since they are well known, their principles of operation have been extensively presented in the literature, and therefore, no relative information is given here. For further implementation details, the reader can refer to the literature.<sup>20–23</sup> Among several parameters a GA uses, the most important ones refer to the population size ( $P_s$ ), the number of generations ( $G_n$ ), the crossover rate ( $C_r$ ), and the mutation rate ( $M_r$ ). These parameters are given here the following values:  $P_s = 80$ ,  $G_n = 100$ ,  $C_r = 0.75$ , and  $M_r = 0.05$ .

## 4 | RESULTS, DISCUSSION, AND FURTHER INVESTIGATIONS

### 4.1 | Design results

Eighteen sets of design results were derived (3 methods x 3 objective functions x 2 rotor topologies). For the inner rotor topology, Table 1 shows the optimization results of the 12 design variables through FMC, GA, and PS and for each one of the cost functions applied ( $CF_1$ – $CF_3$ ). Table 2 shows the same results for the outer rotor topology. For demonstration purposes, some of the optimized designs obtained (objective function  $CF_3$ ) were visualized and are depicted in Figures 3 and 4, with respect to (w.r.t.) their geometry and their flux density distribution. From these tables and figures, it is initially clear that all algorithms succeeded to satisfy all of the existing constraints and to converge to a near-optimum design solution. As an example, the motor's outer diameter is kept within satisfactory limits (24–42 cm, with a 20- to 50-cm constraint), while the machine length lies mainly in the 10- to

**TABLE 1** Results of PMSM design variables through FMC, GA, and PS optimization methods (inner rotor)

		FMC			GA			PS		
		$CF_1$	$CF_2$	$CF_3$	$CF_1$	$CF_2$	$CF_3$	$CF_1$	$CF_2$	$CF_3$
$N_m$		60	62	32	72	60	20	60	62	36
$N_{spp}$		0.48	0.50	0.38	0.561	0.233	0.999	0.742	0.288	0.48
$D_o$	(cm)	25.63	28.25	37.60	24.41	28.74	37.66	27.54	28.00	29.45
$D_{rc}$	(cm)	20.00	20.00	21.50	20.00	20.24	26.15	20.00	20.00	20.02
$L$	(cm)	10.80	10.00	15.60	10.00	11.79	10.01	10.00	14.94	19.32
$n_s$		14	10	13	11	10	20	10	10	10
$l_m$	(mm)	8.35	15.00	15.00	7.50	7.40	10.50	11.40	6.40	5.50
$b_{ts}$	(mm)	4.05	2.50	8.20	2.50	9.70	8.60	3.00	5.40	4.00
$h_{ss}$	(mm)	9.20	15.50	41.70	9.00	21.40	22.10	12.70	20.00	25.10
$h_{sw}$	(mm)	2.00	2.50	13.00	2.00	4.80	5.00	4.20	2.00	4.30
$k_{open}$		0.49	0.357	0.20	0.609	0.802	0.236	0.9	0.254	0.20
$\delta$	(mm)	3.0	3.0	3.0	3.0	3.0	3.9	7.3	3.5	4

Abbreviations: FMC, Fmincon; GA, genetic algorithm; PMSM, permanent magnet synchronous motor; PS, pattern search.

**TABLE 2** Results of PMSM design variables through FMC, GA, and PS optimization methods (outer rotor)

		FMC			GA			PS		
		$CF_1$	$CF_2$	$CF_3$	$CF_1$	$CF_2$	$CF_3$	$CF_1$	$CF_2$	$CF_3$
$N_m$		72	58	46	60	78	60	26	46	26
$N_{spp}$		0.64	0.34	0.44	0.472	0.190	0.477	0.435	0.48	0.683
$D_o$	(cm)	24.91	42.18	25.10	25.56	31.16	33.45	31.30	34.48	37.77
$D_{rc}$	(cm)	24.00	25.31	23.60	23.83	27.99	27.52	29.12	32.85	35.06
$L$	(cm)	10.00	10.00	15.00	10.00	10.01	10.00	10.00	11.02	12.49
$n_s$		10	14	15	13	10	10	10	10	10
$l_m$	(mm)	8.80	7.10	5.00	9.00	7.40	5.00	14.30	10.80	6.40
$b_{ts}$	(mm)	2.50	3.70	8.80	4.40	8.70	2.80	17.30	7.80	9.90
$h_{ss}$	(mm)	6.00	14.30	10.00	10.00	15.80	12.10	14.60	10.80	13.50
$h_{sw}$	(mm)	1.00	1.00	4.70	3.10	4.00	2.00	4.70	4.00	4.70
$k_{open}$		0.90	0.233	0.89	0.574	0.2	0.694	0.9	0.314	0.9
$\delta$	(mm)	6.4	3.0	3.0	4.2	3.0	5.1	14.4	4.2	15.2

Abbreviations: FMC, Fmincon; GA, genetic algorithm; PMSM, permanent magnet synchronous motor; PS, pattern search.

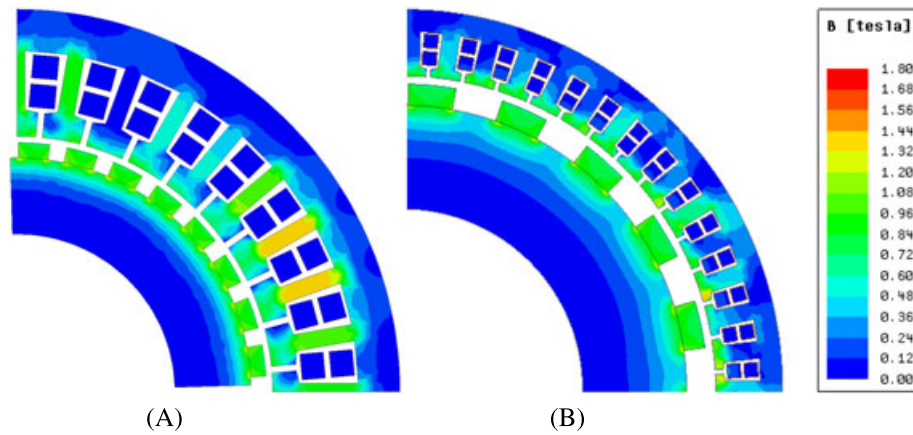


**FIGURE 3** Typical design optimization results obtained. Geometry and flux density distribution for inner rotor topology and  $CF_3$  objective function: A, Fmincon. B, genetic algorithm

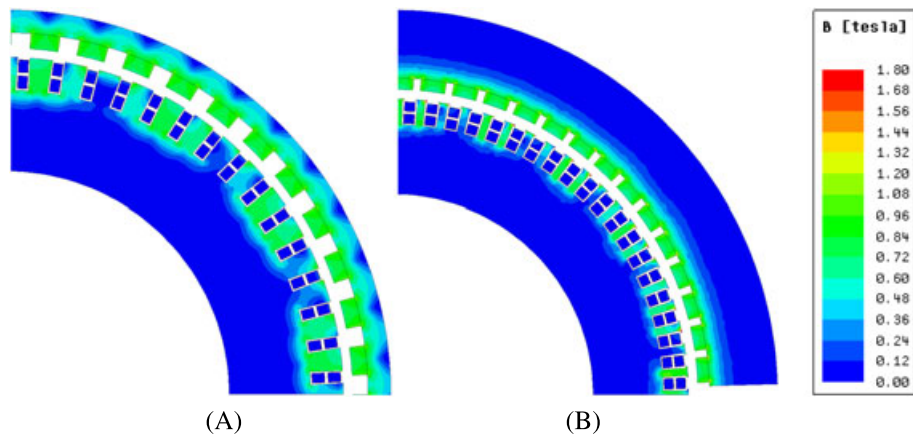


**FIGURE 4** Typical design optimization results obtained. Geometry and flux density distribution for outer rotor topology and  $CF_3$  objective function: A, Fmincon. B, genetic algorithm

**TABLE 3** Objective quantities results through FMC, GA, and PS optimization methods (inner rotor)

	FMC			GA			PS		
	$CF_1$	$CF_2$	$CF_3$	$CF_1$	$CF_2$	$CF_3$	$CF_1$	$CF_2$	$CF_3$
$M_w^{tot}$ , kg	52.99	68.07	94.41	53.46	73.46	96.11	56.30	89.30	122.47
$\eta$ , %	79.20	86.40	76.50	79.10	82.1	74.80	77.20	82.70	76.34
$M_m^{tot}$ , kg	4.24	5.47	3.04	3.54	3.11	1.93	4.02	3.50	2.25

Abbreviations: FMC, Fmincon; GA, genetic algorithm; PS, pattern search.

**TABLE 4** Objective quantities results through FMC, GA, and PS optimization methods (outer rotor)

	FMC			GA			PS		
	$CF_1$	$CF_2$	$CF_3$	$CF_1$	$CF_2$	$CF_3$	$CF_1$	$CF_2$	$CF_3$
$M_w^{tot}$ , kg	22.50	49.53	32.58	22.10	31.30	27.48	23.50	46.78	52.48
$\eta$ , %	79.77	89.05	78.06	80.63	87.56	76.38	74.41	85.93	71.40
$M_m^{tot}$ , kg	4.58	3.06	2.39	4.10	5.24	2.41	3.19	5.30	2.14

Abbreviations: FMC, Fmincon; GA, genetic algorithm; PS, pattern search.

12-cm region with a 10- to 50-cm constraint (with a single exception of 19 cm). The maximum magnetic flux density, in any part of the machine, is also found to be around 1.1 T

(with a 1.6 T constraint) for all cases, except the outer rotor configuration optimized by PS where it was 1.3 T, but even in that case the constraint was met. More compact

information can be found in Tables 3 and 4, where the total weight of the PMSM; its efficiency and the total magnets

**TABLE 5** Computational cost (seconds) of optimization methods applied

	Inner Rotor			Outer Rotor		
	$CF_1$	$CF_2$	$CF_3$	$CF_1$	$CF_2$	$CF_3$
FMC, s	2.241	2.604	2.012	2.136	2.173	2.276
GA, s	10.356	9.295	9.789	9.596	8.115	9.112
PS, s	5.476	5.299	5.286	5.341	5.529	5.126

Abbreviations: FMC, Fmincon; GA, genetic algorithm; PS, pattern search.

**TABLE 6** Slot current density (A/cm<sup>2</sup>) results of the 18 designs

	Inner Rotor			Outer Rotor		
	$CF_1$	$CF_2$	$CF_3$	$CF_1$	$CF_2$	$CF_3$
FMC	690	534	315	873	820	608
GA	737	590	240	503	480	395
PS	800	577	223	583	569	551

Abbreviations: FMC, Fmincon; GA, genetic algorithm; PS, pattern search.

weight are shown for inner and outer rotor geometries, respectively, (for the 3 cost functions and through the 3 algorithms used). It is seen that the quantities ranges (min-max) found are 22 to 122 kg, 71.4% to 89.05%, and 1.9 to 5.3 kg. These tables reveal that if, for example, the machine weight is the primary objective (cost function  $CF_1$ ), the outer rotor topology is the choice, with the GA “showing the way” by presenting an efficient (approximately 80%) and very light (approximately 22 kg) motor, while keeping the magnet weight low enough (approximately 4 kg) as seen in Table 4. The second place goes to FMC method applied to the same geometry, while for the PS method, it can be said that fails to present satisfactory results of the same degree. In the case where the magnets weight is the primary objective (cost function  $CF_3$ ), the same conclusions are true. Indeed, GA presents a solution with quite satisfactory efficiency (approximately 76.4%), low magnet weight (2.4 kg), while keeping the total machine weight low (approximately 27.5 kg), as also shown in Table 4. Fmincon provides the second “alternative” again,

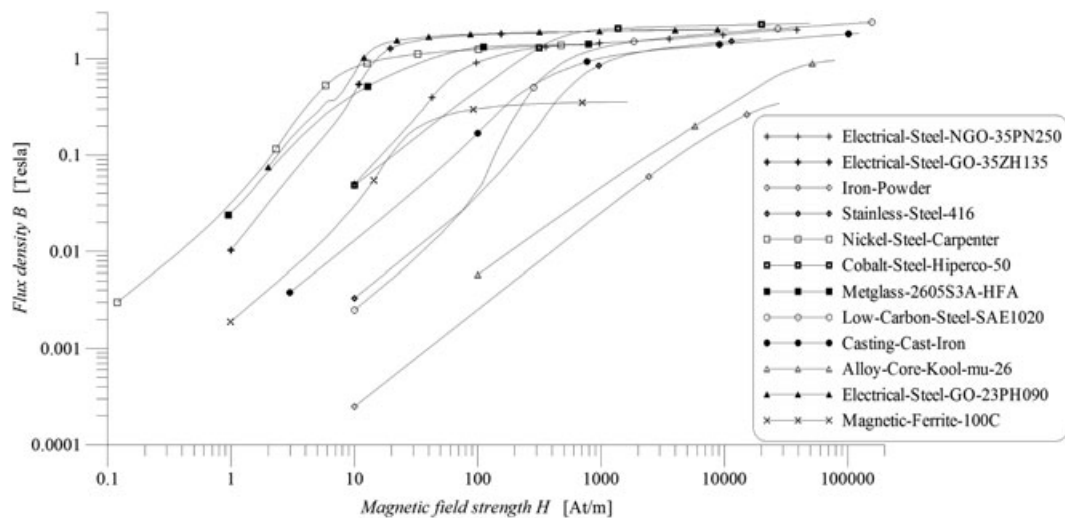


**FIGURE 5** B-H curves of the 12 additional (and commercially available) materials used here for permanent magnet synchronous motor stator and rotor cores

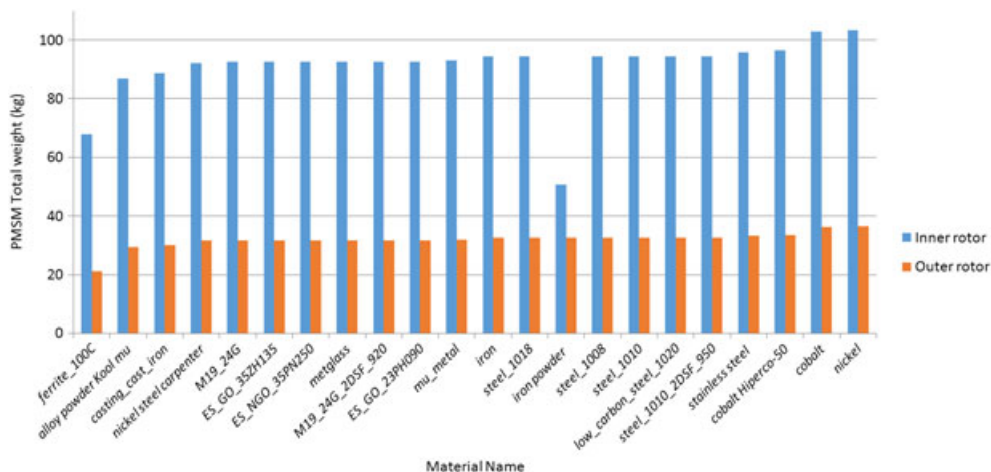


**FIGURE 6** Effect of ferromagnetic materials (for stator and rotor cores) on optimized permanent magnet synchronous motor's (PMSM's) weight for inner and outer rotor topologies (optimization method Fmincon, cost function  $CF_3$ )



while PS method presents quite heavy machines in this case. The computational costs of the adopted and applied methods to PMSM optimization problem are shown in Table 5. Here, FMC method comes first by providing solutions in the order of magnitude of about 2 seconds for the specific problem. Pattern search method is spending almost 2.5 times more computational time, and finally, GA is the slowest optimization method with a response time of approximately 10 seconds.

Finally, Table 6 summarizes the thermal calculations results involving the slot current density for each one of the geometries found. As stated in Section 2.4, only 2 (outer rotor)

cases need force cooling, while the rest of 16 topologies can be manufactured as air-cooled machines.

## 4.2 | Effect of different ferromagnetic materials

The results obtained previously were calculated by incorporating M19\_24G as the stator and rotor core material and NdFe35 type for the PMs. M19\_24G is a silicon nonoriented (its magnetic properties are practically the same in any direction of magnetism in the plane of the material) electrical steel. It is commonly used in large generator, motors, and transformers, as it has superior permeability at high induc-

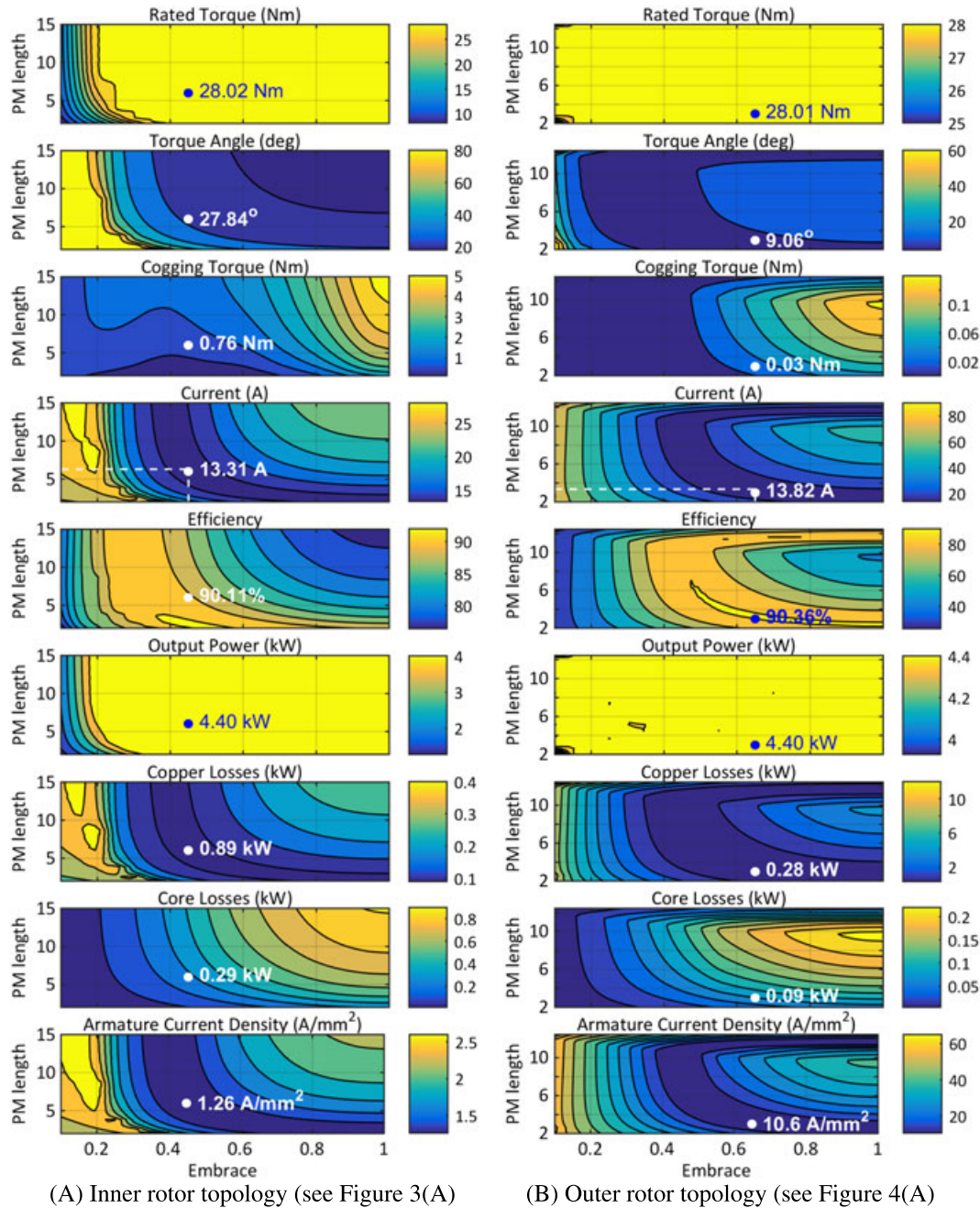


**FIGURE 7** Effect of variation of pole-arc per pole-pitch ratio  $\beta$  (x-axis to all subgraphs) and magnet length  $l_m$  (y-axis to all subgraphs) on 9 quantities of optimized permanent magnet synchronous motor with Fmincon method and cost function  $CF_3$ . A, Inner rotor topology (see Figure 3A). B, Outer rotor topology (see Figure 4A). PM, permanent magnet

tions, low average core losses, and good gauge uniformity and allows high values of stacking factor to be achieved during manufacturing. Keeping the magnet type the same, another consideration was examined, which relates to the choice of soft ferromagnetic materials from which the cores could be constructed. It can be said that this is a “mandatory” step towards to the industrial application of any PMSM derived result.

In every case, the same material was tested for both cores. We consider the geometries of the third cost function ( $CF_3$ ) optimized with FMC method (Figures 3A and 4A) since we choose that the magnet weight is of primary concern,

mainly because of its cost. Moreover, since this cost function presents solutions with low PM weights and at the same time high total machine weights, the effect of several materials consideration is more rigid. It should be noted though that without loss of generality of the design process shown here, any appropriately formulated cost function may be applied.

Based on the above, the analysis took place with the application of 22 different materials. Ten of them were available through the commercial softwares database used, while the rest 12 were processed and incorporated by the authors. For the updating of the softwares database, the authors made an

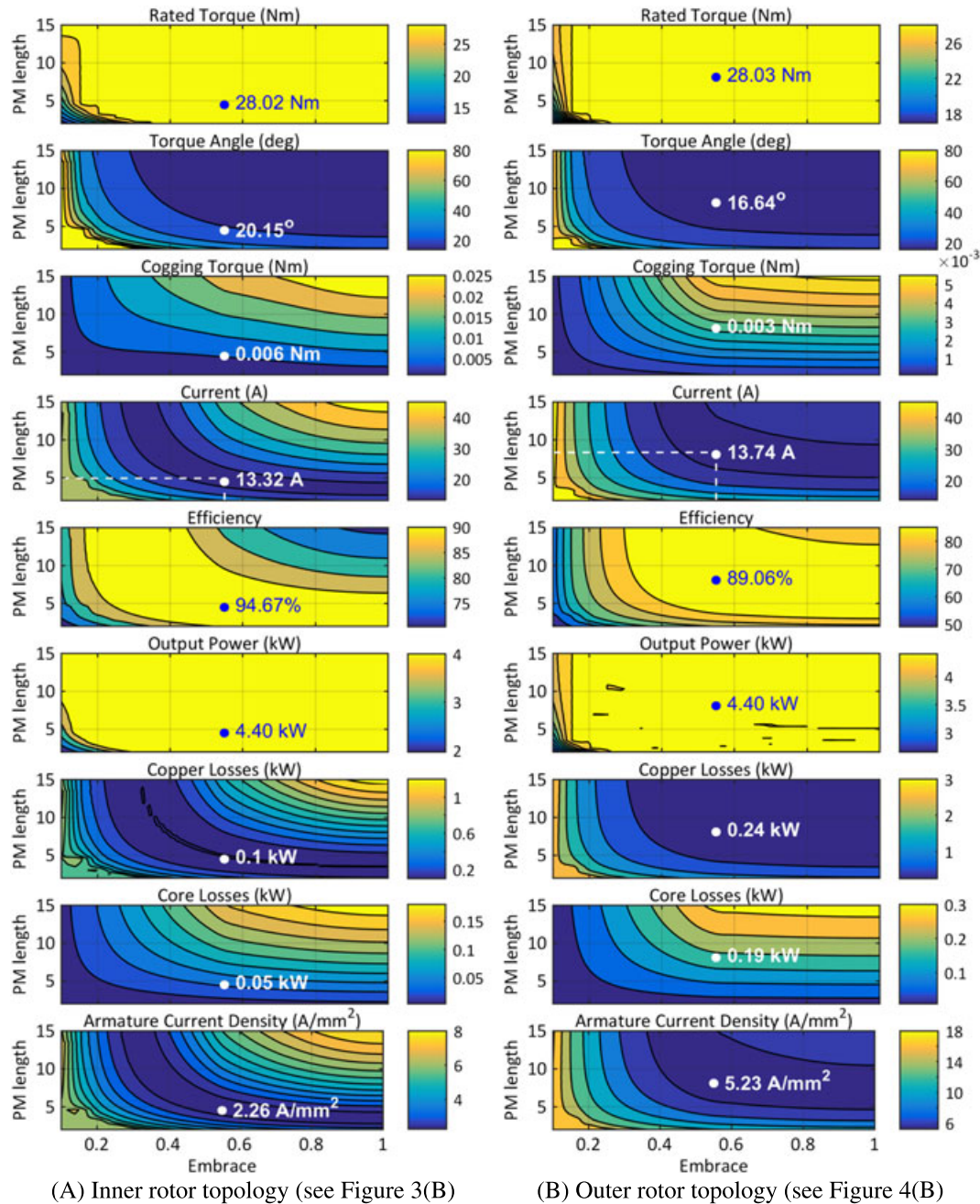


**FIGURE 8** Effect of variation of pole-arc per pole-pitch ratio  $\beta$  (x-axis to all subgraphs) and magnet length  $l_m$  (y-axis to all subgraphs) on 9 quantities of optimized permanent magnet synchronous motor with genetic algorithm method and cost function  $CF_3$ . A, Inner rotor topology (see Figure 3B). B, Outer rotor topology (see Figure 4B). PM, permanent magnet



effort to retrieve real data from commercially available materials in the free market<sup>24</sup> and secondly proceed with data entry of the relative B-H curves of these materials as well as their properties, ie, bulk conductivity, mass density, using the software capabilities.<sup>25</sup> For reference reasons, the B-H curves of the new (added) materials (along with their commercial names) are shown in Figure 5. By using one of the materials each time, simulations were performed and the values of (1) the efficiency, (2) the output torque, and (3) the total weight of the PMSM were recorded. It was noticed that all of the materials achieved the required torque as well as

the predefined efficiency. This is commented as an expected feature since the energy density of the magnets used is high enough. Therefore, Figure 6 depicts only the total machine weight recordings, where the material performance has been sorted out from lower to higher values. It can be seen that there are 9 materials that score lower machine weight values than that of the M19\_24G initially used. Based on that, from a manufacturer's point of view, the material commercial cost is another crucial affecting factor in order for the machine designer to make an appropriate choice for a certain application.

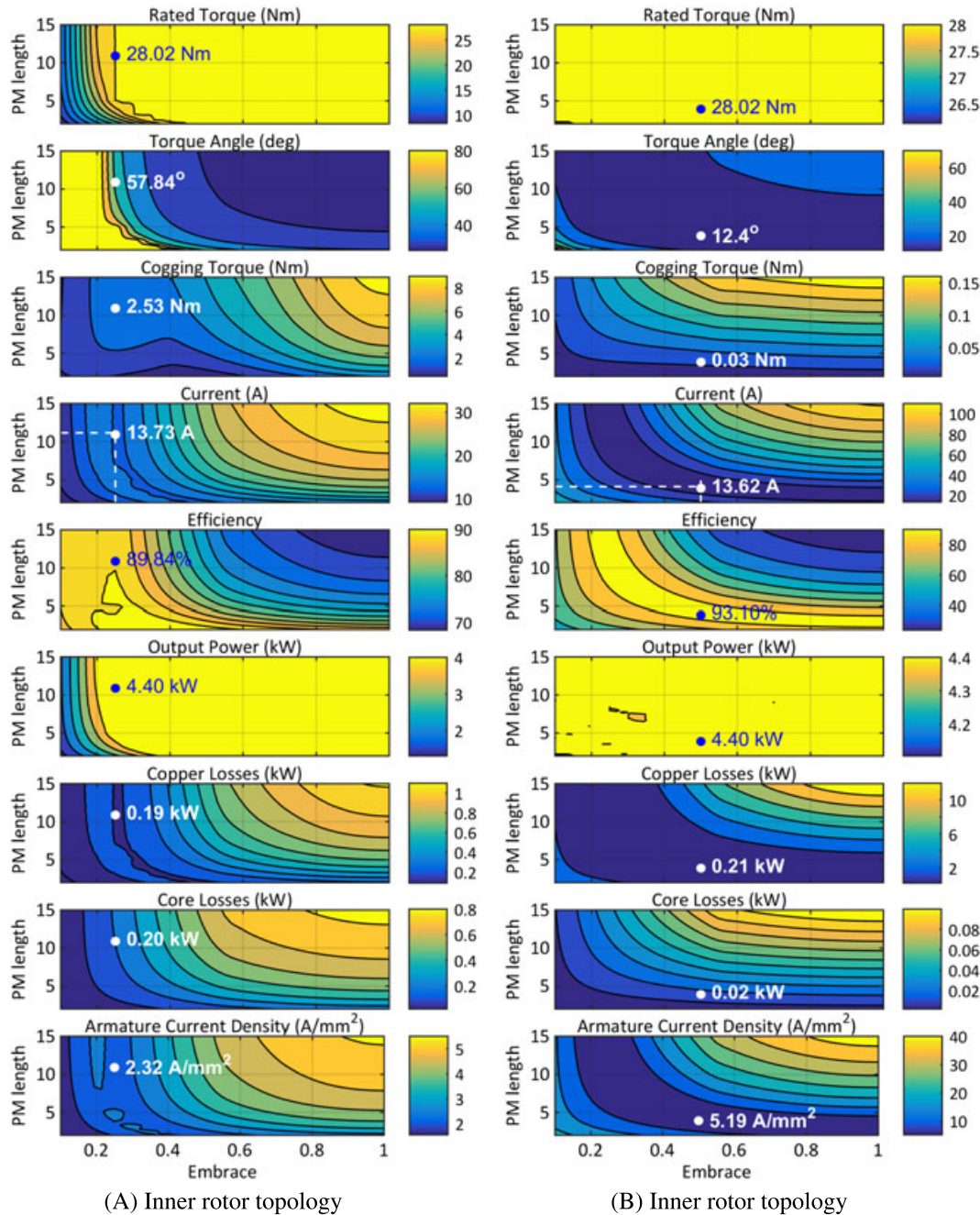


**FIGURE 9** Effect of variation of pole-arc per pole-pitch ratio  $\beta$  (x-axis to all sub-graphs) and magnet length  $l_m$  (y-axis to all sub-graphs) on 9 quantities of optimized permanent magnet synchronous motor with pattern search method and cost function  $CF_3$ . A, Inner rotor topology. B, Outer rotor topology. PM, permanent magnet

**TABLE 7** Optimum combinations of embrace and magnet length (first 2 rows) for minimum PM weight and PMSM current and relative performance quantities

Quantity	Method→ Rotor→	FMC		GA		PS	
		Inner	Outer	Inner	Outer	Inner	Outer
Best embrace, %		<b>45.0</b>	<b>65.0</b>	<b>55.0</b>	<b>55.0</b>	<b>25.0</b>	<b>50.0</b>
Best magnet length, mm		<b>6.45</b>	<b>3.35</b>	<b>4.95</b>	<b>8.55</b>	<b>11.35</b>	<b>4.35</b>
Rated torque, Nm		28.02	28.01	28.02	28.03	28.02	28.03
Torque angle, deg		27.84	9.06	20.15	16.64	57.84	12.40
Cogging torque, Nm		0.762	0.034	0.006	0.003	2.528	0.029
Root Mean Square (RMS) line current, A		13.31	13.82	13.32	13.74	13.73	13.62
Current density, A/mm <sup>2</sup>		1.26	10.60	2.26	5.23	2.32	5.19
Magnet weight, kg		2.511	1.742	1.758	2.993	2.547	2.161
Total PMSM weight, kg		98.05	32.34	52.23	38.50	61.72	55.86
Iron losses, kW		0.293	0.088	0.048	0.195	0.204	0.019
Copper losses, kW		0.089	0.281	0.100	0.246	0.193	0.207
Efficiency, %		90.11	90.36	94.67	89.06	89.84	93.10

Abbreviations: FMC, Fmincon; GA, genetic algorithm; PM, permanent magnet; PMSM, permanent magnet synchronous motor; PS, pattern search.

### 4.3 | Effect of pole-arc per pole-pitch ratio and magnet length

The results obtained and presented in the previous paragraphs solve the initial formulated problem and satisfy the constraints set. The last phase of this work considers the influence of pole-arc per pole-pitch ratio ( $\beta$ ) and magnet length ( $l_m$ ) variation (see Figure 1A) on PMSM performance. Nine quantities were chosen as “focus points,” namely, efficiency, magnet weight, output torque, torque angle, cogging torque, line current, iron losses, armature copper losses, and armature current density. The cores material was set back to M19\_24G and  $\beta$  varied from 0.1 to 1.0 with a step of 0.05, while  $l_m$  varied from 2.0 to 15 with a step of 0.05, giving a total of 4959 simulations for each topology (with 1 exception of 3990 simulations in a case where the magnet length could not exceed 12.45 mm due to outer stator diameter and air-gap). Therefore, for the 6 topologies a total of 28 785 simulations were conducted.

The magnet weight is also of primary concern here so the 6 relevant ( $CF_3$ ) optimized topologies were chosen. Since there are ( $x, y, z$ ) triples results in this analysis, contour plots of the aforementioned quantities as a function of  $\beta$  and  $l_m$  were chosen to be depicted in Figures 7 to 9.

It can be seen that each geometry configuration presents unique formulation of these contours for each quantity. In turn, the goal was to find the “best combination” of  $\beta$  and  $l_m$  in such a way that the optimum design can be finally met. For this goal, an analysis performed by sorting out the results in ascending order for the magnets weight (we recall here that we are examining  $CF_3$  and the cost of the magnets is of concern) and at the same time in ascending order for the PMSMs current (since we are interested in economical long-term motor operation). The first 2 rows of Table 7 shows the best combinations found, while the rest of it summarizes the “focus” quantities values as they are affected, for every topology examined. From this table (as well as from Figures 7–9), it can be observed that since the designs have

been preoptimized already, the desired rated torque and output power are almost always satisfied for any of  $\beta$  and  $l_m$  combination. Also, for easy reference purposes, a “dot” sign following by its corresponding value has been assigned to all subgraphs of Figures 7 to 9. The best combination chosen actually exhibits the minimum motor line current (for maximum economic operation), while at the same time, the corresponding magnet weight can be considered as the minimum necessary quantity which ensures the desired nominal specifications during this economic operation. From a “decision-making” point of view, it is concluded that the inner rotor configuration preoptimized by GA method (Table 1) combined with best  $\beta$  and  $l_m$  values of Table 7 presents the most attractive solution among the others. It exhibits low torque angle, low cogging torque, low current density, low magnet weight, low enough machine weight, low iron and copper losses, and the highest efficiency. Finally, it should be noted that the investigation, which took place in this subsection is judged as a necessary stage (refinement) in the modelling and optimization procedure proposed here, since the pole-arc to pole-pitch parameter has not been taken into account in the analytical calculation stage described in Section 2 and to which all methods adopted were based on.

## 5 | CONCLUSIONS

The paper presented, analyzed, and discussed the modelling approach of a multiobjective optimization problem, related to the radial flux PMSM with inner and outer rotor topologies for low-speed direct drive applications. Three optimization algorithms were adopted, applied, and evaluated find (as a case study) competitive alternative designs to replace traditional low-speed induction motor/gearbox systems. An easy to modify weighted multiobjective function has also been proposed and an effort was made to categorize and present briefly the large but necessary amount of problem variables, constant

and constraints. Using an analytical procedure, a stable convergence observed on the optimization results regarding the solution sets of 12 main problem design variables. Several ferromagnetic core materials were also applied regarding the optimized PMSMs designs. Moreover, the effect of the magnets embrace and length variations was considered through parametric investigations, leading to improved designs. The overall derived results using the analytical, FEM, and parametric calculations revealed clearly, that a multiobjective PMSM optimization has to be modelled and performed carefully in cases where certain quantities are of primary concern.

## REFERENCES

- Vogel K, Rossa AJ. Improving efficiency in AC drives: comparison of topologies and device technologies. *Proceedings of Intl. Exhibition and Conference for Power Electronics, Intelligent Motion, Renewable Energy and Energy Management*, PCIM, Nuremberg, Germany; May 20-22, 2014:509–516.
- Waide P, Brunner C. Energy-efficiency policy opportunities for electric motor-driven systems. *Intl. Energy Agency (IEA) Working Paper*, Paris, France (www.iea.org); 2011:11–17.
- Meier F. Permanent magnet synchronous machines with non-overlapping concentrated windings for low speed direct drive applications. *PhD Thesis*, Royal Institute of Technology, KTH, Stockholm, 2008.
- Libert F, Souillard J. Design study of a direct driven surface mounted permanent magnet motor for low speed application. *Proceedings of Intl. Symposium on Advanced Electromechanical Motion Systems*, vol. 2, Marrakesh, Morocco; 2003:1–6.
- Ficheux R, Caricchi F, Crescimbeni F, Onorato H. Axial-flux permanent magnet motor for direct-drive elevator systems without machine room. *IEEE Trans Ind Appl*. 2001;37(6):1693–1701.
- Spooner E, Williamson AC. Direct coupled permanent magnet generators for wind turbine applications. *IEE Proc - Electr Power Appl*. 1996;143(1):1–8.
- Dubois MRJ. Optimized Permanent Magnet Generator Topologies for Direct-Drive Wind Turbines. *PhD Thesis*, TU Delft, Delft University of Technology, 2004.
- Chen JY, Nayar CV, Longya X. Design and finite-element analysis of an outer rotor permanent magnet generator for directly coupled wind turbines. *IEEE Trans Magn*. 2000;36(5):3802–3809.
- Eriksson S, Bernhoff H, Bergkvist M. Design of a unique direct driven PM generator adapted for a telecom tower wind turbine. *Renewable Energy*. 2012;44:453–456.
- Krøvel Ø, Nilssen R, Skaar SE, Løvli E, Sandøy N. Design of an integrated 100kW permanent magnet synchronous machine in a prototype thruster for ship propulsion. *Proceedings of 16th Intl. Conf. Electrical Machines*, ICEM, Cracow, Poland; 2004:cd.ref. 697.
- Xianglin L, Kwok CT, Ming C. Analysis, design and experimental verification of a field-modulated permanent-magnet machine for direct-drive wind turbines. *IET Electr Power Appl*. 2015;9(2):150–159.
- Karnavas YL, Korkas CD. Optimization methods evaluation for the design of radial flux surface PMSM. *Proceeding of Intl. Conf. on Electrical Machines*, ICEM, vol. 1, Berlin, Germany; 2014:1348–1355.
- Pyrhonen J, Jokinen T, Hrabovcova V. *Design of Rotating Electrical Machines*, 2. Somerset, NJ, USA: John Wiley & Sons; 2013.
- Hassan W, Bingsen W. Efficiency optimization of PMSM based drive system. *Proceedings of IEEE Intl. Conf. on Power Electronics and Motion Control*, IPEMC, vol. 1, Harbin, China; 2012:1027–1033.
- Magnussen F, Sadarangani C. Winding factors and Joule losses of permanent magnet machines with concentrated windings. *Proceedings of IEEE Intl. Conf. on Electric Machines & Drives*, vol. 1, Madison, Wisconsin; 2003:333–339.
- Dorell DG. Combined thermal and electromagnetic analysis of permanent-magnet and induction machines to aid calculation. *IEEE Trans Ind Electron*. 2008;55(10):3566–3574.
- Hendershot JR, Miller TJE. *Design of Brushless Permanent Magnet Machines*. 2nd ed.: Motor Design Books LLC; 2010.
- Ponmurugan P, Rengarajan N. Multi-objective optimization of electrical machine, a state of the art study. *Int J Comput Appl*. 2012;56(13):26–30.
- ITT Flygt, Product catalogue, mixing products section (low speed). Available from: <http://www.flygt.com/>, Accessed on 10 Dec 2015.
- Optimizations Toolbox™ User's Guide. MA, USA: Matlab Release R2013b, The Mathworks Inc; 2013.
- Mitsuo G, Runwei C. *Genetic Algorithms and Engineering Optimization*. Canada: John Wiley & Sons; 2000.
- Eiben AE, Ráú PE. Genetic algorithms with multi-parent recombination. *Proceedings of Intl. Conf. on Parallel Problem Solving from Nature*, LNCS, vol. 866. Springer-Verlag; 1994:78–87.
- Audet C, Dennis Jr JE. Analysis of generalized pattern searches. *SIAM J Optim*. 2003;13(3):889–903.
- Magnetic Material Database MagWeb. Available from: <http://magweb.us/>, Accessed on 4 Jan 2016.
- ANSYS Electromagnetic Suite (EM) v16: Maxwell 2D/3D User's Guide; 2015.

**How to cite this article:** Karnavas Y, Chasiotis I, Korkas C, Amoutzidis S. Modelling and multi-objective optimization analysis of a permanent magnet synchronous motor design. *Int J Numer Model*. 2017;e2232. <https://doi.org/10.1002/jnm.2232>

## APPENDIX

### Problem Parameters

**TABLE A1** Induction motor-gearbox data corresponding to PMSM

Quantity	Symbol	Induction Motor	Gearbox	Total	PMSM	Unit
Outer stator diameter	$D_o$	18	50	50	50	cm
Machine length	$L$	9.5	40.5	50	50	cm
Machine weight	$M_w^{tot}$	22	131	153	150	kg
Efficiency	$\eta$	88	90	79	79	%
Shaft torque	$T$	28	1:30	840	840	Nm
Shaft speed	$n$	1500	30:1	50	50	rpm
Output power	$P_{out}$	4.4		4.4	4.4	kW
Line current	$I$	8.6		8.6	8.6	A

Abbreviation: PMSM, permanent magnet synchronous motor.



**TABLE A2** Design search variables and their universe of discourse

Quantity	Symbol	Variable Range	Unit
No. of magnet poles	$N_m$	20-80	
No. of slots/pole/phase	$N_{spp}$	0.001-1	
Outer stator diameter	$D_o$	20-50	cm
Outer rotor diameter	$D_{rc}$	$\ 20 - D_o\ $	cm
Active machine length	$L$	10-50	cm
No. of slot conductors	$n_s$	10-40	
Magnet thickness	$l_m$	2-15	mm
Stator tooth width	$b_{ts}$	2.5	mm
Stator slot height	$h_{ss}$	0	mm
Slot wedge height	$h_{sw}$	$1 - h_{ss}$	mm
bs0/bss1 ratio	$k_{open}$	0.2-0.9	
Airgap length	$\delta$	3-20	mm

**TABLE A3** Values of the constants involved in the design procedure

Quantity	Symbol	Set Value	Unit
Maximum flux density (NdFeB)	$B_{max}$	1.6	tesla
Remanence flux density	$B_r$	1.08	tesla
Area occupied by conductors	$k_{cp}$	0.25	
Operating frequency	$f$	50	Hz
Relative permeability	$\mu_r$	1.03	
Motors shaft speed	$n$	50	rpm
Mass density of the copper	$P_{copper}$	8920	kg/m <sup>3</sup>
No. of phases	$N_{ph}$	3	
Mass density of the back iron	$P_{bi}$	7750	kg/m <sup>3</sup>
Copper resistivity	$\rho_{Cu}$	$1.72 \times 10^{-8}$	$\Omega/m$
Mass density of the magnet	$P_m$	7500	kg/m <sup>3</sup>
Torque on the motors shaft	$T$	840	Nm

**TABLE A4** Constraints of the PMSM design problem

Description	Symbol	Constraint
Stator yoke height	$h_{sy}$	$\geq h_{ss}/2$
Slot wedge height	$h_{sw}$	$\geq 1$ mm
Slot opening height	$h_{s0}$	$\geq 2$ mm
Slot width	$b_{ss2}$	$0.15h_{ss} \leq b_{ss2} \leq 0.5h_{ss}$
Tooth width	$b_{ts}$	$\geq 0.3r_s$
Slot opening width	$b_{ss0}$	$\geq 2$ mm
Flux density in stator teeth	$B_{ts}$	$\leq 1.6$ T
Flux density in stator yoke	$B_{sy}$	$\leq 1.4$ T
Flux density in rotor yoke	$B_{ry}$	$\leq 1.4$ T
Air-gap flux density	$B_{\delta}$	$\leq 1.1$ T
Copper losses	$P_{Cu}$	$\leq 700$ W
Magnet weight	$M_m^{tot}$	$\leq 5.5$ kg
Machine weight	$M_w^{tot}$	$\leq 150$ kg

Abbreviation: PMSM, permanent magnet synchronous motor.